

Response to Anonymous Referee RC 2

We thank the referee for the careful reading and the useful comments and will adapt the manuscript accordingly. Below is a point by point reply with the referee's comments in bold font, our reply in italic font and the changes in manuscript in normal font.

Comment of the referee:

MAJOR COMMENT: The open ocean generation of baroclinic Rossby waves requires two fundamental elements: time-dependence of the atmospheric forcing and perturbations of the ocean thermocline. The latter are produced by the vertical Ekman pumping associated with the horizontal divergence of the Ekman transport, which, in turn, is proportional to the vertical component of the curl of the surface wind stress So I wonder why the authors have chosen the zonal wind stress tau1 instead of curl(tau) as the representative observable for the atmosphere. Their choice is even more surprising because, to investigate the synchronization they analysed “the vertical motion of the isopycnals” induced by Rossby waves in the KE region; this is absolutely correct but, then, why ignoring the same effect in the open ocean where the waves are generated? In my opinion the best thing would be to redo all the calculations starting from curl(tau) instead of tau1. Alternatively, I recommend to calculate the first PC of the vertical component of curl(tau), compare it with Fig. 2d and show that the two time series are, in their turn, fairly well synchronized. This is possible; in fact, if on the one hand, in the extreme -unrealistic- case of latitude-independent zonal wind stress no wave generation would occur, on the other hand, some degree of synchronization between the first PC of tau1 and that of curl(tau) can be expected. In any case I strongly recommend the authors to address this important issue.

Author's reply:

We have redone the phase synchronization analysis using the wind stress curl. In particular, we calculated the first PC of the wind stress curl in a PCA which is shown in Fig. 1d. After smoothing, it is similar to the one obtained for the zonal wind stress. The EOF pattern of the wind stress curl (Fig. 1b) is different to the one obtained for the zonal wind stress and the variance for the first EOF of the wind stress curl (7.6%) is much smaller compared to the zonal wind stress (29.6%). The spectrum of the first PC of the wind stress curl $\nabla \times \tau_M(t)$ (Fig. 2b) still shows a dominant period of 8 years. Afterwards, a SSA was applied to the first PC of the wind stress curl. The same dominant period of 8 years was found. The corresponding ST-PCs pair consist of ST-PC 3 and 4 (for the zonal wind stress the ST-PC pair associated with a period of 8 years this was 1-2) and is indicated in Fig. 2d & f. For the ST-PCs pair 3-4 the reconstructed component $\nabla \times \tau_M(t)$ was calculated. Note that the results of the SSA are given for a lag of $M = 325$ months in the case of the wind stress curl while for the zonal wind stress results were given for a lag of $M = 375$ months.

As a next step, a two-dimensional embedding of $\nabla \times \tau_M(t)$ with its Hilbert transform was done. Oscillations of the trajectory in the plane spanned by the (time derivative) of $\nabla \times \tau_M(t)$ and its Hilbert transform around the origin can be observed (Fig. 3b).

Results for the phase synchronization analysis are shown in Fig. 3c & d for the $\nabla \times \tau_M(t)$ and the $L_M(t)$ (i.e. the time series obtained after performing a SSA for the KE path length). Fig. 3c shows the phase difference evolution between $L_M(t)$ and $\nabla \times \tau_M(t)$ for three lag-window lengths ($M = 275, 325$ and 365 months). As for the zonal wind stress, a (significant) plateau can be identified between model year 200 and 240 for all three values of M indicating a phase synchronization. Epochs with plateaus in the phase difference evolution are confirmed by the statistical test using a sliding window of 120 months length (Fig. 3d). The phase synchronization between model year 200 and 240 occurs for various values of lags M . For lags $M > 340$ Fig. 3d also reveals a plateau for model years 250 to 290.

All in all, using the wind stress curl in the phase synchronization analysis resulted in very similar results as for the zonal wind stress with some minor changes such as the precise ST-PCs pair.

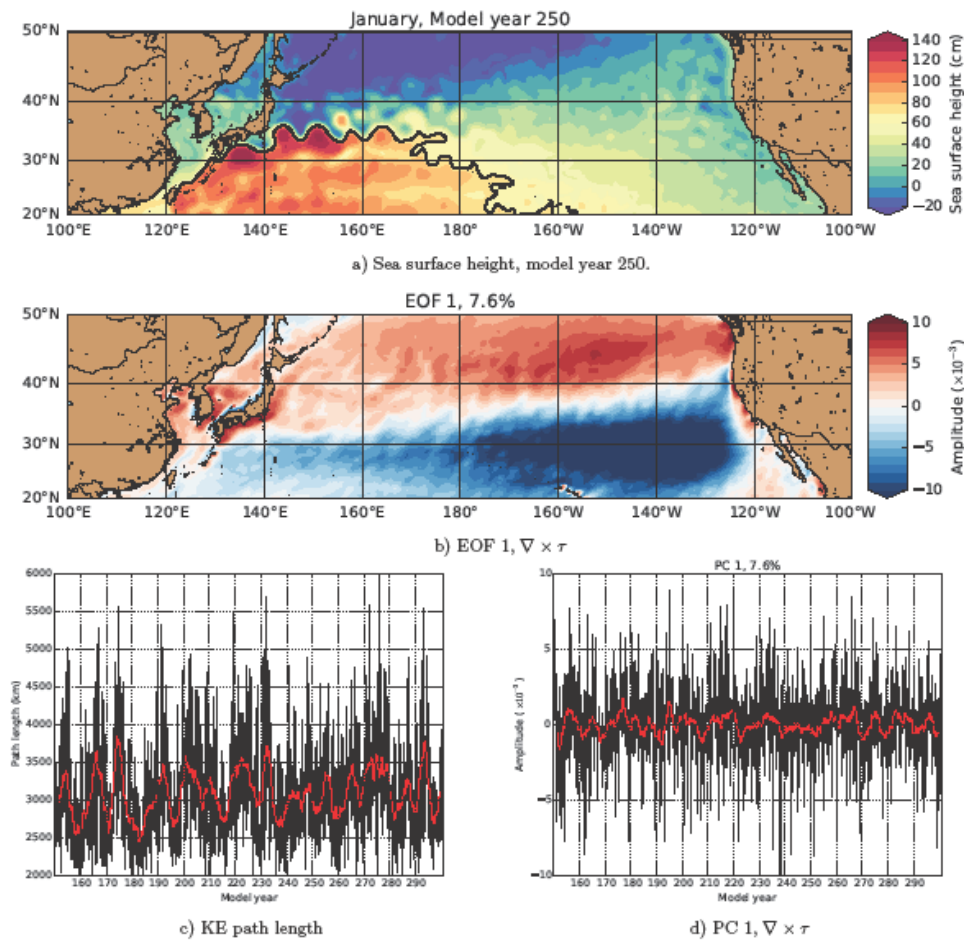


Figure 1: Sea surface height field in the North Pacific basin for January model year 250. The black curve is the 70 cm SSH isoline that represents the KE jet. (b): First EOF of the wind stress curl over the North Pacific basin, explaining 7.6 % of the total variance. (c): Time series of the KE path length along the region 140°E – 60°E, together with its moving average of 36 months (red curve). (d): First PC of the wind stress curl over the North Pacific basin, together with its moving average of 36 months (red curve).

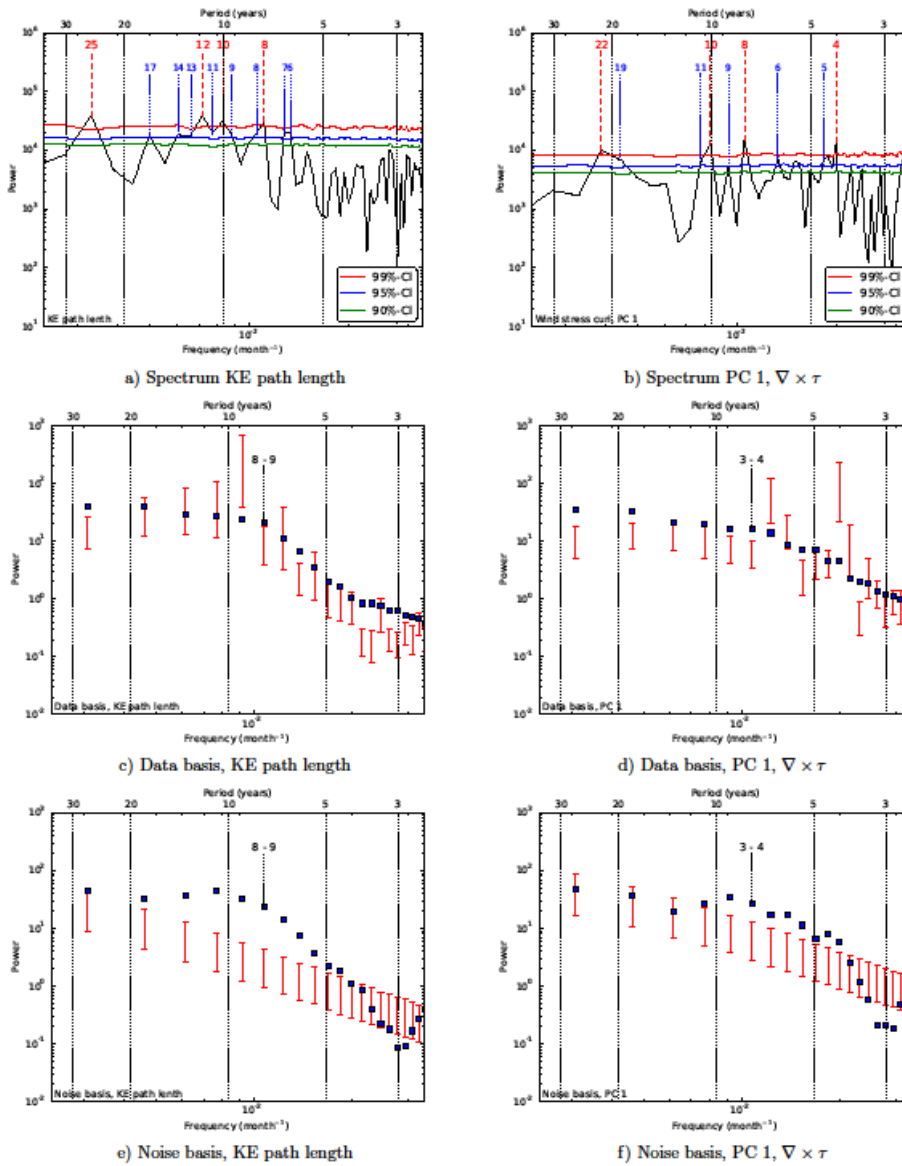


Figure 2: (a & b): Fourier spectrum (black curve) of the KE path length and the first PC of the wind stress curl. The colour-coded curves are the significance levels of red noise surrogates, where the number (in years) indicate significant periods. (c & d): Data basis from the Monte Carlo SSA for the KE path length and the first PC of the wind stress curl. (e & f): Noise basis from the Monte Carlo SSA for the KE path length and the first PC of the wind stress curl. SSA was performed with a total lag of 325 months and for the Monte Carlo SSA 2500 realizations have been used. The 95% confidence intervals which have been calculated from the surrogates are shown by the red vertical bars. A specific ST-PC is represented by the blue markers and is associated with a certain frequency. The ST-PCs related to the 8-year period are significant in both the data basis and the noise basis (Allen & Robertson, 1996) and the ST-PC pair related to this variability is indicated.

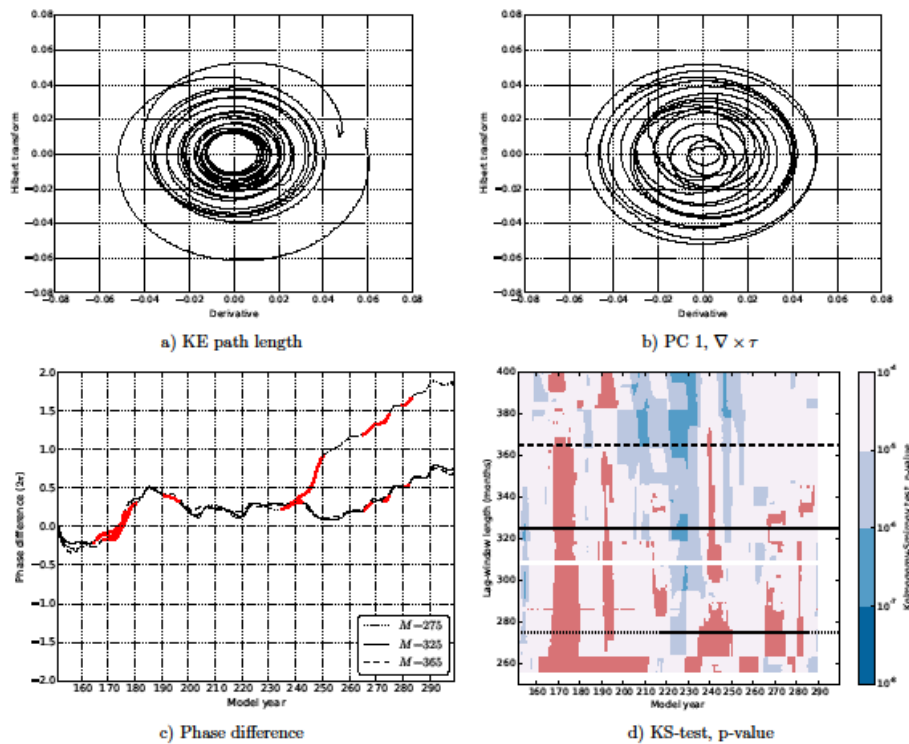


Figure 3: (a & b): Embedding of the time derivative of the KE path length time series $L_M(t)$ (a) and that of the first PC of the wind stress curl (b) by the Hilbert transformation. (c): Phase difference between $L_M(t)$ and $\nabla \times \tau_M(t)$ for three lag-window lengths M . The black curves indicate starting points of the sliding window (length of 120 months) with p -value < 0.0001 . Intervals that are not significant (p -value ≥ 0.0001) are indicated in red. The black horizontal lines indicate the values of M used in (c).

Changes in text:

A remark on the similarity of the phase synchronization analysis for the zonal wind stress and the wind stress curl will be added.

MINOR COMMENTS

Comment of the referee:

The mathematical method used in the analysis is relatively complex and requires the implementation of several steps, so it is not easy to follow the description. Besides, the listing of the technical steps does not end in sect. 2.2. but continues in sect. 3.1 on the variability. In particular, it is difficult to follow lines 8-30 of page 7. Therefore I suggest to compact the discussion of all the technical details in sect. 2.2 and to add a flowchart summarizing the mathematical technique. This would be very helpful, especially because I believe that the Hilbert method does not belong to the typical background of oceanographers.

Author's reply:

Section 2.2. aims to give a general introduction to the main method used to study phase synchronization effects including the Hilbert transform to derive the phase of the time series, the calculation of the phase difference as well as the statistical test to determine (statistically significant) epochs of phase synchronization. In Section 3.1. information on the processing (detrending, removing the seasonal cycle, and SSA) of the time series chosen as representatives for the proposed synchronizing processes (i.e. for which the phase synchronization analysis introduced in Section 2.2. will be done) is given and their variability is described. We agree that it might be confusing that the information on the processing of the time series is given after the introduction of the phase synchronization method (which comes later in the work flow).

Changes in text:

We will reorganize the description of the technical steps given in Section 2.2. and Section 3.1. to clarify the methods used to study the Kuroshio Current system.

In addition, we will add further explanations of the Singular Spectrum Analysis and its parameters in the text.

Comment of the referee:

p. 1, l. 22-24: the description of the elongated KE mode corresponds to that of the contracted mode, and vice versa, please exchange.

Author's reply:

Agreed.

Changes in text:

The text will be changed to "An ~~elongated~~ contracted (~~contracted~~ elongated) state is characterized by...".

Comment of the referee:

p. 2, l. 15-16: I do not think a critical effect of topography has been recognized to determine "An intensified mesoscale eddy field". Please provide references.

Author's reply:

Qiu & Chen (2010) describe that a southward shift of the KE jet results in interactions with the shallow topography of the Shatsky Rise which eventually leads to an increase of the eddy kinetic energy state of the KE system west of the Shatsky Rise. As a consequence of the intensified mesoscale eddy field, the southern recirculation gyre is strengthened.

Changes in text:

We will provide the corresponding references for this statement.

Comment of the referee:

p. 3, l. 9-11: I do not fully agree with the sentence: ": : focussing on what we think is a missing piece to reconcile the forced and internal views as sketched above: a phase synchronisation of the KCS variability with the zonal wind-stress variability in the North Pacific". Such phase synchronization has indeed been investigated in several modelling studies, several of them also quoted by the authors. I would therefore suggest to use a more moderate sentence, and similarly elsewhere.

Author's reply:

We agree that modelling studies with the aim to reconcile the forced and the internal view on the KCS variability exist and also provide an investigation of the relation between the wind stress and KCS variability. On the other hand, an explicit framing of the KCS variability in terms of phase synchronization as it is described in section 5.2 of Pikovsky et al. (2001) and especially using the corresponding method from nonlinear dynamics (phase difference evolution and the statistical test) to address the phase synchronization cannot be found. In addition, in the meantime we were pointed to work by Andrew Kiss (Kiss and Frankcombe, 2016, J. Clim) where they study synchronization mechanisms (between time dependent wind stress and western boundary current response) in idealized QG models.

Changes in text:

We will adjust the statement (and similar statements elsewhere) to account for the existing modelling studies and clarify the difference to our contribution by the phase difference approach used. We will also include the work using idealized models.

Comment of the referee:

p. 4, l. 8: define the path length parameter in the text (now it is defined only in the caption to Fig. 1) and discuss why it has been chosen among the many available parameters applied to the KE variability in previous studies.

Author's reply:

The KE path length is derived from the 70 cm SSH isoline along the region 140°E – 160°E. The respective isoline can be identified in the sea surface height field in the North Pacific basin displayed in Fig.1. The path length was shown to be a very good indicator of the different KCS states in many previous studies (Qiu & Chen, 2010, Pierini et al., 2009) and is therefore chosen.

Changes in text:

The definition of the KE path length given in the caption of Fig.1 is indirectly given in the text (p. 4, l. 7). We will change the respective sentence to “In CESM, the KE path length is based on the 70-cm SSH contour in the region along 140°E – 160°E”. We will more clearly motivate the use of the KE path length as a parameter for the KE variability on p. 4 (where the two time series representing the processes which are supposed to synchronize are introduced).

Comment of the referee:

p. 12, l. 12-14: “The travel time of these Rossby waves from the eastern to the western side of the North Pacific basin is estimated to be roughly 10 years corresponding to the observed decadal variability of the Kuroshio oscillator.” First of all the travel time of 10 years is much large than that observed by several authors (which is of 2-3 years). Secondly, the decadal variability of the KCS may be linked to that of the atmosphere but not to the travel time of the waves. Please clarify the first point and reformulate the sentence.

Author's reply:

We do not agree. In the original Chelton and Schlax (Science 2008) paper, typical Rossby wave travel times at 30 N are about 10 years.

Changes in text:

The reference to the Chelton and Schlax 2008 paper will be included and a remark on the time scale will be made.

Comment of the referee:

Section 4 includes, summary, discussion and conclusions. I think it would be much better to move the discussion about some crucial points (e.g., p. 14, l. 19-24, 28-31) in section 3.3.

Author's reply:

Section 4 is structured as following: The first paragraph summarizes the goal and main results of the study. Then the phase synchronization and its coupling / forcing mechanism is addressed. In this context, it is discussed why the processes are not synchronized during the whole model time and an explanation is proposed (related to the strength of the forcing). This could, of course, also be discussed in the section 3.2. The next paragraph focuses on the Rossby waves and give climatologically forced model results as a supporting argument for the mechanism of synchronization. Finally, an outlook is given on the demonstration of the synchronization phenomenon using real data.

Changes in text:

As further explanations / clarifications related to p. 14 l. 19-24 will be added to Section 4 (Comments of Referee 1) we will consider whether it will be appropriate to reorganize parts of Section 4.

Comment of the referee:

p. 13, l. 16: his -> is

Author's reply:

Agreed.

Changes in text:

Text will be changed to "The optimal-lag correlation ~~his~~ is expected to occur at about 1/2 of the mean oscillation period, which is about 4 years, consistent with Figure 6b."